Recent Results from HERA

S. Glazov

DESY, Notkestraße 85, 22607 Hamburg, Germany

HERA *ep* collider provides unique information on the proton structure. High center-of-mass energy $s = 320$ GeV gives access to both the low Bjorken-x domain and regime of high momentum transfers Q. An ultimate precision for the deep inelastic scattering cross section is achieved by combining the measurements of the H1 and ZEUS collaborations. The combined data are used as a sole input to a QCD fit to obtained HERAPDF set. Both collaborations report measurements of the structure function F_L which provides important check of the QCD evolution. Semi-inclusive analyzes give additional information on the strong couplin constant α_S and heavy flavor contribution.

1 Introduction

Deep inelastic lepton-hadron scattering (DIS) is important for the understanding of the structure of the proton and of the dynamics of parton interactions. The discovery of Bjorken scaling [1] and its violation [2] at fixed target experiments triggered the development of the theory of strong interactions, Quantum Chromodynamics (QCD). Significant progress in the exploration of strong interactions has been achieved at the electron-proton collider HERA.

The high center-of-mass energy of the *ep* scattering at HERA leads to a wide kinematic range extending to large values of the absolute of the four-momentum transfer squared, Q^2, and to very small values of the Bjorken x variable. Electron (proton) beam energy of $E_e = 27.6\,\mathrm{GeV}$ ($E_p = 920\,\mathrm{GeV}$) give access to Bjorken x values as small as 10^{-4} for Q^2 of $10\,\mathrm{GeV}^2$ and Q^2 values as high as $30000\,\mathrm{GeV}^2$ for high x. A QCD analysis of the inclusive cross-section data allows to determine parton distribution functions (PDFs).

HERA operation spanned over 15 years, from 1992 until 2007, with a shutdown in 2000−2002 to upgrade luminosity and instal spin rotators, to enable longitudinal beam polarization for the colliding experiments. The two colliding experiments, H1 and ZEUS, collected the DIS data for the whole HERA running period. The data before the luminosity upgrade is used for high precision measurements at low Q^2 and low x, where the scattering cross section is high. The data after the luminosity upgrade is focused more on high Q^2 analyzes and polarization studies. For the last three months of its operation HERA run at reduced proton beam energy to measure the proton structure function F_L.

2 DIS Cross Section

The neutral current deep inelastic $e^{\pm}p$ scattering cross section, at tree level, is given by a linear combination of generalized structure functions. For unpolarized beams it can be expressed as

$$\sigma^{\pm}_{r,\mathrm{NC}} = \frac{\mathrm{d}^2\sigma^{\pm}_{\mathrm{NC}}}{\mathrm{d}x\mathrm{d}Q^2} \cdot \frac{Q^4 x}{2\pi\alpha^2 Y_+} = \tilde{F}_2 \mp \frac{Y_-}{Y_+}x\tilde{F}_3 - \frac{y^2}{Y_+}\tilde{F}_L, \tag{1}$$

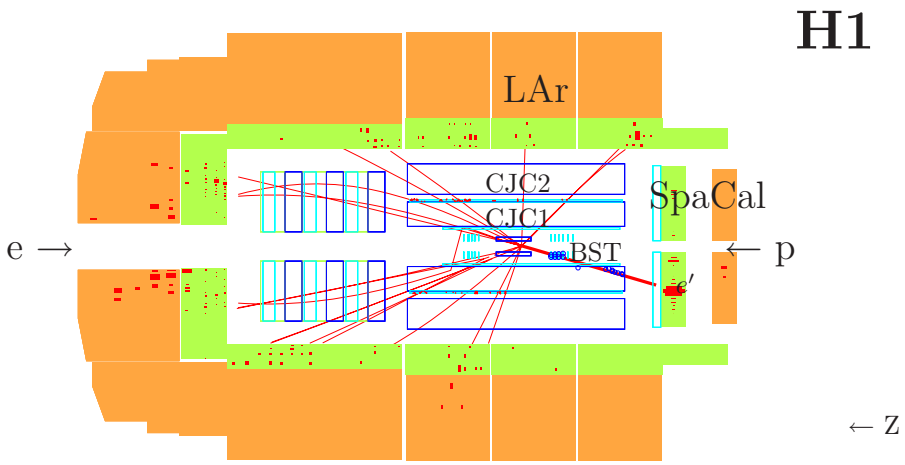

Figure 1: A view of a high y event reconstructed in the H1 detector. The positron and proton beam directions are indicated by the arrows. For the coordinate system used at HERA the z axis points in the direction of the proton beam. The interaction vertex is reconstructed using the hadronic final state (thin lines) and the scattered positron (thick line) tracks in the central tracker. The central tracker consists of (from the beam line outwards) the silicon tracker, the drift chambers CJC1 and CJC2, it is surrounded by the liquid argon (LAr) calorimeter. The detector operates in a solenoidal magnetic field of 1.16 T. The scattered positron trajectory is reconstructed in the backward silicon tracker BST and the CJC1. The charge of the particle is determined using the track curvature. The positron energy is measured in the electromagnetic part of the SpaCal calorimeter.

where the electromagnetic coupling, the photon propagator and a helicity factor are absorbed in the definition of a reduced cross section $\sigma^{\pm}_{r,\mathrm{NC}}$, and $Y_{\pm} = 1 \pm (1-y)^2$. The functions $\tilde{F}_2$, $\tilde{F}_L$ and $x\tilde{F}_3$ depend on the electroweak parameters as:

$$\begin{aligned} \tilde{F}_2 &= F_2 - \kappa_Z v_e \cdot F_2^{\gamma Z} + \kappa_Z^2 (v_e^2 + a_e^2) \cdot F_2^Z, \\ \tilde{F_L} &= F_L - \kappa_Z v_e \cdot F_L^{\gamma Z} + \kappa_Z^2 (v_e^2 + a_e^2) \cdot F_L^Z, \\ x\tilde{F}_3 &= \kappa_Z a_e \cdot xF_3^{\gamma Z} - \kappa_Z^2 \cdot 2 v_e a_e \cdot xF_3^Z. \end{aligned} \tag{2}$$

Here v_e and a_e are the vector and axial-vector weak couplings of the electron to the Z boson and $\kappa_Z(Q^2) = Q^2/[(Q^2 + M_Z^2)(4\sin^2\Theta\cos^2\Theta)]$. At low Q^2, the contribution of Z exchange is negligible and $\sigma_{r,\mathrm{NC}} = F_2 - y^2 F_L / Y_+$. The contribution of the term containing the structure function F_L is only significant for large values of y.

In the Quark Parton Model (QPM) the structure function F_L is zero [3] and the other functions in equation 2 are given as

$$\begin{aligned} (F_2, F_2^{\gamma Z}, F_2^Z) &= [(e_u^2, 2e_u v_u, v_u^2 + a_u^2)(xU + x\bar{U}) \\ &+ (e_d^2, 2e_d v_d, v_d^2 + a_d^2)(xD + x\bar{D})], \\ (xF_3^{\gamma Z}, xF_3^Z) &= 2x[(e_u a_u, v_u a_u)(xU - x\bar{U}) \\ &+ (e_d a_d, v_d a_d)(xD - x\bar{D})], \end{aligned} \tag{3}$$

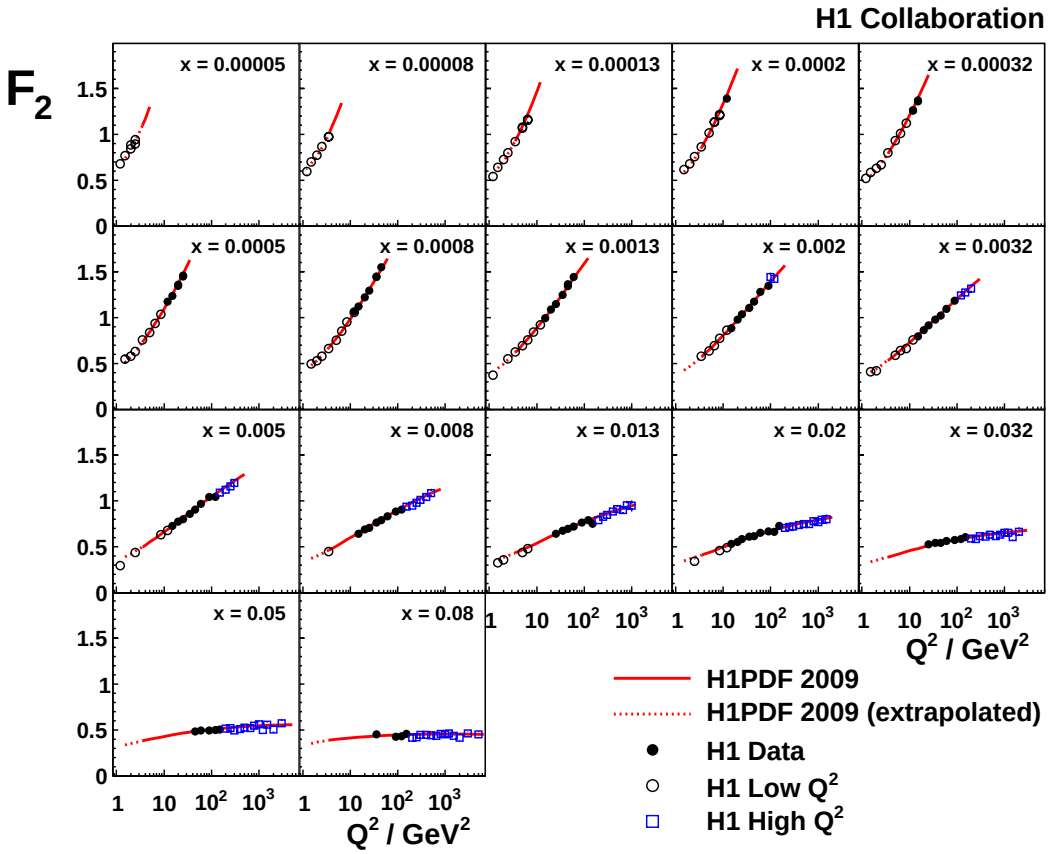

Figure 2: Measurement of the structure function F_2 as a function of Q^2 at various values of x by the H1 collaboration. The error bars represent the total measurement uncertainties. The solid curve represents the H1PDF 2009 QCD fit for $Q^2 \geq 3.5$ GeV^2, which is also shown extrapolated down to $Q^2 = 1.5$ GeV^2 (dashed).

where e_u, e_d denote the electric charge of up- or down-type quarks while $v_{u,d}$ and $a_{u,d}$ are the vector and axial-vector weak couplings of the up- or down-type quarks to the Z boson. Here xU, xD, $x\overline{U}$ and $x\overline{D}$ denote the sums of up-type, of down-type and of their anti-quark distributions, respectively. Below the b quark mass threshold, these sums are related to the quark distributions as follows

$$\begin{array}{ll} xU = xu + xc, & x\overline{U} = x\overline{u} + x\overline{c}, \\ xD = xd + xs, & x\overline{D} = x\overline{d} + x\overline{s}\,, \end{array} \tag{4}$$

where xs and xc are the strange and charm quark distributions. Assuming symmetry between sea quarks and anti-quarks, the valence quark distributions result from

$$xu_v = xU - x\overline{U}, \qquad xd_v = xD - x\overline{D}. \tag{5}$$

A reduced cross section for the inclusive unpolarized charged current $e^{\pm}p$ scattering is

$$\sigma^{\pm}_{r,\mathrm{CC}} = \frac{2\pi x}{G_F^2}\left[\frac{M_W^2 + Q^2}{M_W^2}\right]^2 \frac{\mathrm{d}^2\sigma^{\pm}_{\mathrm{CC}}}{\mathrm{d}x\mathrm{d}Q^2}. \tag{6}$$

At leading order, the e^+p and e^- charged current scattering cross sections are

$$\begin{aligned} \sigma^{+}_{r,\mathrm{CC}} &= x\overline{U} + (1-y)^2 xD, \\ \sigma^{-}_{r,\mathrm{CC}} &= xU + (1-y)^2 x\overline{D}. \end{aligned} \tag{7}$$

The NC and CC measurements may be used to determine the combined sea quark distribution functions, $\overline{U}$ and $\overline{D}$, and the valence quark distributions, u_v and d_v. A QCD analysis in the DGLAP formalism [4] also allows the gluon momentum distribution xg in the proton to be determined from the scaling violations of the data.

For NC scattering, event kinematics can be reconstructed using the scattered electron as well as the hadronic final state particles. A typical low Q^2, high y event measured by the H1 detector is shown in figure 1. For CC scattering, kinematics is reconstructed using the hadronic final state.

3 Measurements of DIS Cross Section at low Q^2 by H1

Recently the H1 collaboration reported new measurements of the NC cross section at low $0.2 \leq Q^2 \leq 150$ GeV^2 [5, 6] based on data collected in 1999-2000. The precision of the data reaches 1.3% for intermediate values of Q^2. Figure 2 shows the structure function F_2 for fixed values of x as a function of Q^2 obtained from these cross-section results. For low x, there is a strong Q^2 dependence of the structure function. For highest x, the data show approximate scaling behavior. The data are compared to an next-to-leading order (NLO) QCD fit, termed H1PDF2009, which describes the data very well.

4 Combination of the H1 and ZEUS data

The highest precision of the cross-sections measurements at HERA is obtained by combining the results from the H1 and ZEUS experiments. The combination of the results is performed

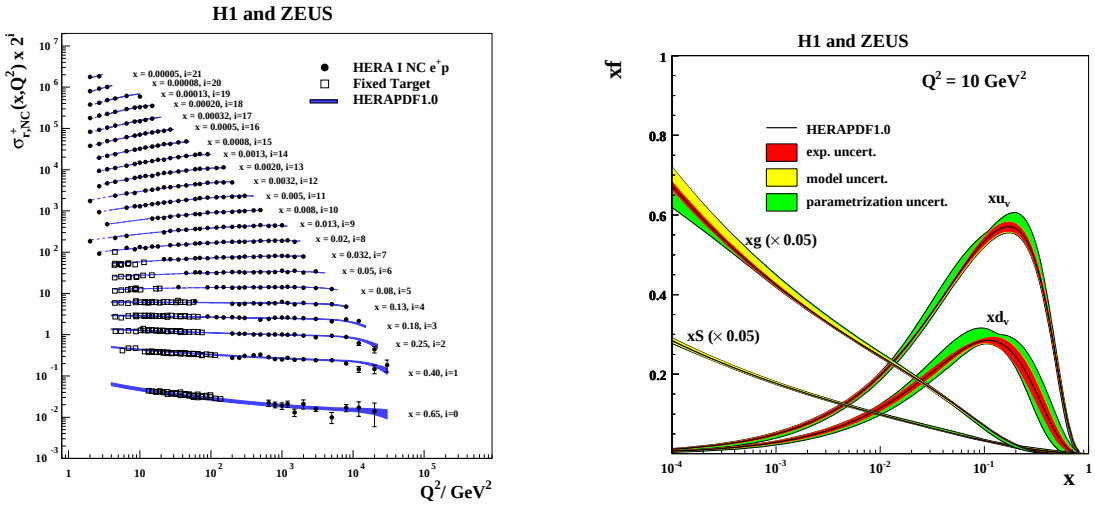

Figure 3: Measurement of the e^+p NC scattering cross section based on the combination of the H1 and ZEUS data compared to the fit to these data and measurements from fixed-target experiments.

taking into account the correlated systematic uncertainties [5, 11]. The starting point is the χ^2 function for individual measurement which is defined as

$$\chi^2_{\rm exp}\left(\boldsymbol{m},\boldsymbol{b}\right) = \sum_i \frac{\left[m^i - \sum_j \gamma^i_j m^i b_j - \mu^i\right]^2}{\delta^2_{i,\rm stat}\,\mu^i\left(m^i - \sum_j \gamma^i_j m^i b_j\right) + \left(\delta_{i,\rm uncor}\,m^i\right)^2} + \sum_j b_j^2\,. \tag{8}$$

Here μ^i is the measured value at a point i and γ^i_j, $\delta_{i,\rm stat}$ and $\delta_{i,\rm uncor}$ are relative correlated systematic, relative statistical and relative uncorrelated systematic uncertainties, respectively. The function $\chi^2_{\rm exp}$ depends on the predictions m^i for the measurements (denoted as the vector $\boldsymbol{m}$) and the shifts of correlated systematic error sources b_j (denoted as $\boldsymbol{b}$). For the reduced cross-section measurements $\mu^i = \sigma^i_r$, i denotes a (x, Q^2) point, and the summation over j extends over all correlated systematic sources. The predictions m^i are given by the assumption that there is a single true value of the cross section corresponding to each data point i and each process, neutral or charged current e^+p or e^-p scattering. Under the assumption that the statistical uncertainties are proportional to the square root of the number of events and that the systematic uncertainties are proportional to $\boldsymbol{m}$, the minimum of equation 8 provides an unbiased estimator of $\boldsymbol{m}$.

Several data sets providing a number of measurements are represented by a total χ^2 function, which is built from the sum of the $\chi^2_{\rm exp}$ functions for each data set e The data averaging procedure allows the rearrangement of the total χ^2 such that it takes a form similar to equation 8.

The averaging procedure is applied to the H1 and ZEUS inclusive data from the HERA-I running period. All the NC and CC cross-section data from H1 and ZEUS are combined in one simultaneous minimization[12]. Therefore resulting shifts of the correlated systematic

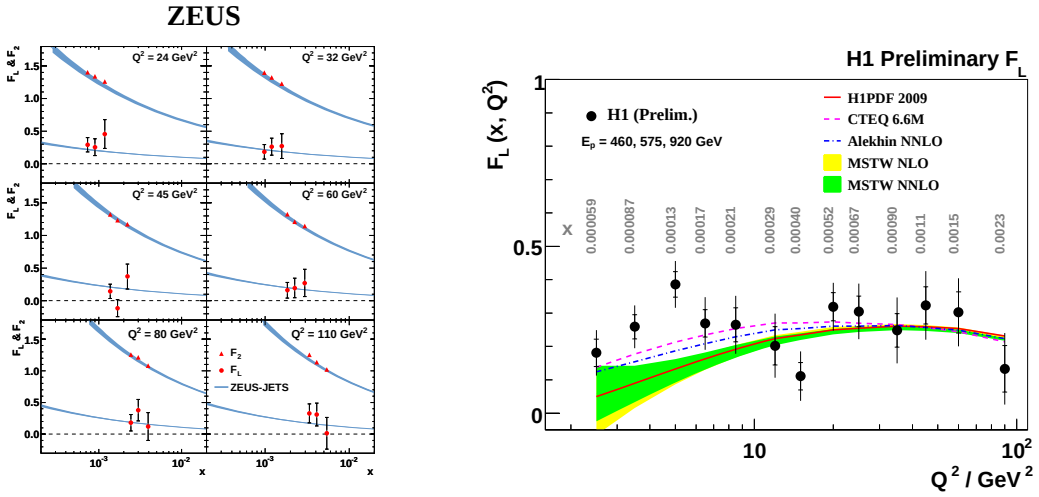

Figure 4: Left: measurement of the structure functions F_L and F_2 by the ZEUS collaboration compared to the prediction of ZEUS-JETS fit. Right: Preliminary measurement of the structure functions F_L and F_2 by the H1 collaboration. The data are quoted at fixed values of Q^2 and x indicated in grey and compared to predictions based on various models.

uncertainties propagate coherently to both CC and NC data. In total 1402 data points are combined to 741 cross-section measurements. The data show good consistency, with $\chi^2/n_{\rm dof} = 637/656$. In figure 3 left, the NC reduced cross section, for $Q^2 > 1\,\text{GeV}^2$, is shown as a function of Q^2 for the HERA combined e^+p data and for fixed-target data [13, 14] across the whole of the measured kinematic plane. The data precision reaches 1.1% for $10 \le Q^2 \le 100$ GeV^2.

The combined data uses as a sole input for the NLO QCD analysis. The result of the fit is compared to the data in figure 3, left. There is a good agreement between the extrapolation of the fit to lower Q^2 and fixed-target data in this kinematic domain. The parton distribution densities obtained in this fit are shown in figure 3, right for $Q^2 = 10$ GeV^2. The QCD analysis considers various sources of the uncertainties which arise from experimental data, model assumptions and parameterization form of the PDFs. A prominent features of the parton densities is the dominance of the gluon and sea at low x.

5 Measurements of the Structure Function F_L

Large gluon density, determined from scaling violation of the F_2 data using QCD fits implies that the structure function F_L must be significant at low x. Direct measurements of F_L allow to test this prediction providing a check of the QCD and adding an extra constraint for the gluon density.

To determine the two structure functions $F_2(x, Q^2)$ and $F_L(x, Q^2)$ from the reduced cross section it is necessary to perform measurements at the same values of x and Q^2 but different y. This is achieved at HERA by reducing the proton beam energy. Two e^+p runs at reduced proton beam energy $E_p = 460$ GeV and $E_p = 575$ GeV were performed with an integrated luminosity of about 13 pb^{-1} and 6 pb^{-1}, respectively. The run at $E_p = 460$ GeV gives highest sensitivity

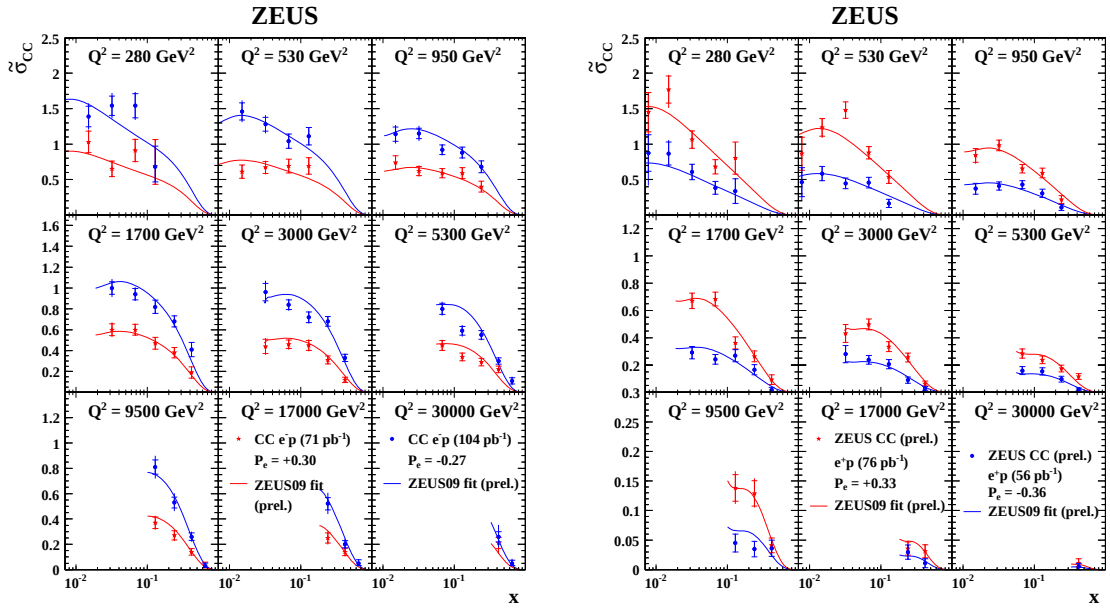

Figure 5: CC e^-p (left) and e^+p (right) scattering cross section measured by the ZEUS collaboration. Data for positive (red stars) and negative (blue dots) polarization are compared to the fit.

to F_L while the run at $E_p = 575$ GeV extends the kinematic range of the measurement and provides an important cross check.

The measurement must extend to as high y as possible to increase sensitivity to F_L. A high y kinematic domain at low Q^2 corresponds to low energies of the scattered positron E'_e. Measurement at low E'_e is challenging primarily because of high hadronic background.

The ZEUS collaboration uses Monte Carlo (MC) simulation to estimate the background. The MC prediction is normalized to the data using a sub-sample of tagged background events. The results of the ZEUS analysis [15] are shown in figure. 4, left. ZEUS report measurement of both structure functions F_2 and F_L obtained from a linear fit of the reduced cross section as a function of y^2/Y_+. The structure function F_L is found to be in a good agreement with the prediction of the ZEUS-JETS PDF set [16].

To reduce and estimate the hadronic background, H1 demand the scattered positron candidate to have a reconstructed track with well measured curvature. The curvature is used to determine the candidate charge. For the signal, positive charge is expected. The background is approximately charge symmetric, i.e. the number of background events with different charges is about equal. Using this, the background is estimated from the negative charge sample, corrected for a small charge asymmetry and then subtracted from the positive charge sample. The charge asymmetry of the background is determined directly from the data by comparing negatively and positively charged candidates from e^+p and e^-p data taking periods, respectively. Therefore, the background determination is purely data driven for the H1 analysis.

H1 published the first measurement of F_L at HERA using drift chambers CJC1 and CJC2 together with the SpaCal calorimeter for $12 \leq Q^2 \leq 90$ GeV^2[17] and also reported a preliminary result at higher Q^2 using the LAr calorimeter [18]. These measurements were recently extended to lower $2.5 < Q^2 < 12$ GeV^2 by using the backward silicon tracker BST [19].

The H1 measurement of the structure function F_L is shown in figure 4, right. The data are compared to the predictions from various models. The predictions agree among each other and with the data for $Q^2 > 10$ GeV^2. For lower Q^2, there is a notable difference between the NLO predictions of MSTW and CTEQ. This difference is traced down to the difference in accounting for α_S^2 corrections. The data are somewhat higher than both predictions and agree better with the CTEQ calculations.

6 Charged Current $e^{\pm}p$ DIS Cross Section

In the standard model, the CC cross section depends linearly on the longitudinal electron beam polarization. Figures 5, left and figures 5, right show published [21] and preliminary analyzes of e^-p and e^+p CC cross sections performed by the ZEUS collaboration. For the published e^-p sample, the same 2005-2006 data are used as for the published NC sample, the preliminary e^+p analysis is based on data collected in 2003-2004 and 2006-2007. The data agree well with the expectations of the QCD fit. The e^+p CC data are of additional value for the QCD analyzes because they are sensitive to the d and s quark densities which are less constraint by the NC data, see equations 3 and 7.

7 Jet Cross Section and Determination of α_S

The production of jets in DIS can be used to determine the gluon density and to measure the strong coupling constant α_S. Recently H1 have performed a measurement of inclusive, 2-jet and 3-jet cross sections [22] as a function of Q^2 using HERA data collected in 1999-2007 with an integrated luminosity of 395 pb^{-1}. The measurements are well described by NLO QCD calculations, corrected for hadronization effects.

Using these data, H1 determine the strong coupling constant α_S. The measurement is performed separately for different Q^2 bins and different processes. These measurements are combined together and the evolution of α_S as a function of Q is compared to the theory prediction in figure 6. A good agreement is observed between the data and theory. The theoretical uncertainty is dominated by the higher order corrections. The value of α_S at M_Z

$$\begin{aligned} \alpha_S(M_Z) &= 0.1176 \pm 0.0020(\text{exp.})^{+0.0046}_{-0.0030}(\text{th.}) \\ &\pm \quad 0.0016(\text{PDF}) \end{aligned} \tag{9}$$

agrees well with the world average. The experimental error on α_S is about 0.6%. The total uncertainty is dominated by the theory, it may be improved with calculation of NNLO corrections.

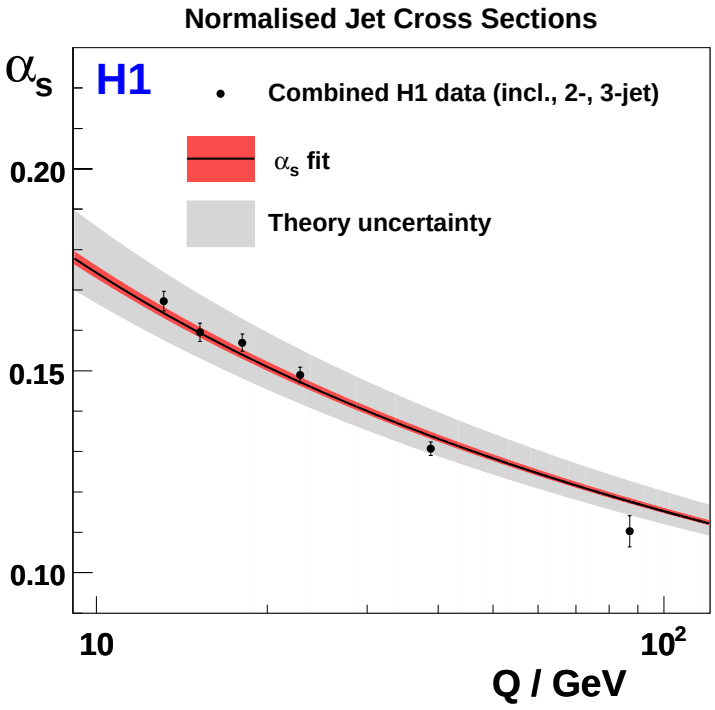

Figure 6: α_S as a function of Q obtained by H1 by a simultaneous fit of all normalized jet cross sections.

8 Measurements of Strange, Charm and Bottom Quark Densities

Inclusive NC cross section at low Q^2 and low x are dominated by the structure function F_2 and do not allow to separate contributions of individual quark flavors. The flavor separation can be achieved in semi-inclusive scattering by tagging the struck quark flavor. For HERA kinematics, tagging production of a charmed meson, e.g. D^*, almost certainly corresponds to a scattering off a c-quark. Samples with secondary vertices are enriched with scattering off c and b-quarks.

To measure b and c structure functions using secondary vertices, it is essential to have high precision tracking detector installed close to the interaction point. Recently the H1 collaboration reported the measurement of c and b reduced cross sections [23], using secondary vertex technique, based on complete sample for which the central silicon tracker was installed. These data are shown in figure 7 and compared to the H1PDF2009 fit. For all Q^2 bins there is a strong rise of the reduced cross section to low x values which increases with increasing Q^2. This is a direct indication of the large gluon density. The data are in a good agreement with the H1PDF2009 fit. The uncertainty of the fit is dominated by the model uncertainty due to the variation of the heavy quark masses. Therefore, these data allow to check the model and determine these parameters.

The fixed-target experiment HERMES, which operated using HERA $e^{\pm}$ beams, recently

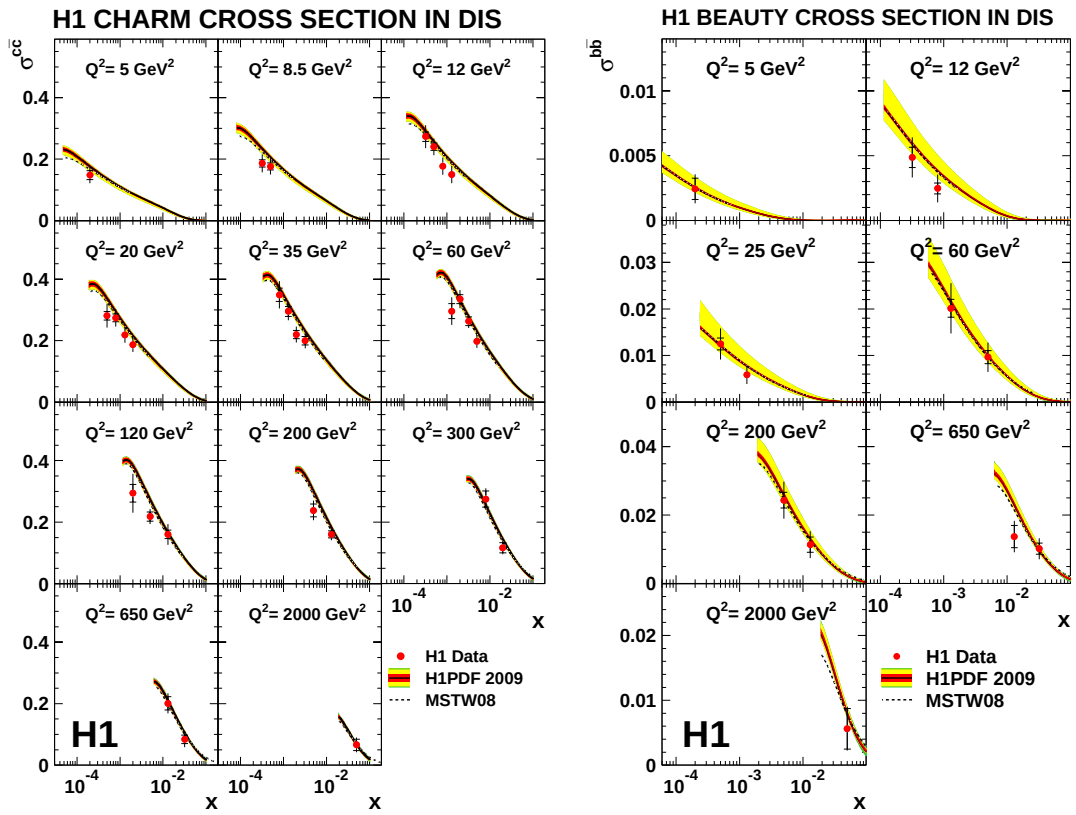

Figure 7: The reduced cross section $\sigma^{c\bar{c}}$ (left) and $\sigma^{b\bar{b}}$ measured by H1 and shown as a function of x for different Q^2 bins. The predictions of H1PDF 2009 and MSTW08 NLO fits to inclusive data are also shown.

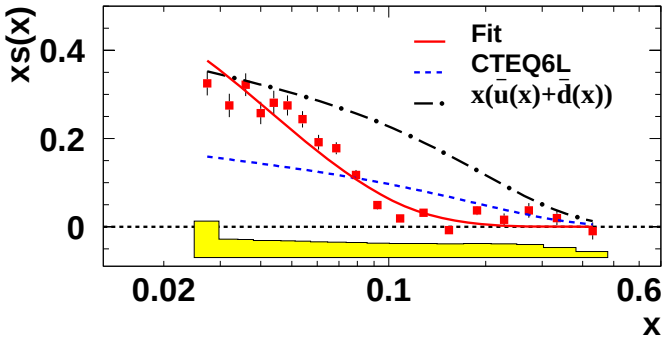

Figure 8: The strange parton distribution $xs(x)$ from the measured HERMES multiplicity for charged kaons evolved to $Q_0^2 = 2.5$ GeV^2 . The solid curve is the HERMES fit to the data, the dashed curve gives $xs(x)$ from the CTEQ6L set, and dot-dashed curve us the sum of light antiquarks from the CTEQ6L set.

reported a measurement of the momentum distribution of the strange quark sea, $xs(x)$, in scattering off deuteron. The strange density is extracted from $K^{\pm}$ multiplicities by correcting for the u, d and s fragmentation. The result is shown in figure 8 and compared to the CTEQ6L expectation. The HERMES data shows softer behavior of $xs(x)$ compared to the CTEQ6L fit: at high x the data is below the fit and at low x the data are above the fit. At low x the strange sea is comparable to the light sea density.

9 Summary

Recent results from HERA provide new precise data for determination of the proton structure at low x. The combination of the H1 and ZEUS results reaches 1.1% for the $10 \leq Q^2 \leq 100$ GeV^2 kinematic domain. The data are well described by the NLO QCD fit. This fit has impressively small experimental uncertainties for the PDFs, the total uncertainties are dominated by the model and parameterization errors.

The conventional QCD picture is checked by the measurements of the structure function F_L performed by H1 and ZEUS. Good agreement between the theory and the measurements is observed for $Q^2 \geq 10$ GeV^2. For lower $2.5 \leq Q^2 < 10$ GeV^2, the preliminary data from H1 are somewhat above the expectations.

Measurements at high Q^2 using the polarized HERA-II data performed by ZEUS check the Standard Model and provide constraints for the parton densities at high x. The flavor decomposition at high x is achieved by using the charged current data.

The flavor decomposition at low x and low Q^2 is performed by measuring semi-inclusive processes: tagged heavy flavor production at H1 and $K^{\pm}$ production at HERMES. The H1 data for the charm and bottom quark parton densities agree well with the predictions from the QCD fit to the inclusive data. The HERMES data are softer than prediction of the CTEQ6L analysis.

Further results from HERA are expected as the data analysis are being finalized. In particular, combined H1 and ZEUS measurements of the inclusive HERA-II cross sections and combined measurement of the charm and bottom production will have significant impact on PDFs for the kinematic range important for the future measurements at the LHC.

References

[1] E.D. Bloom *et al.*, Phys. Rev. Lett. 23 (1969) 930.

[2] D.J. Fox *et al.*, Phys. Rev. Lett. 33 (1974) 1504.

[3] C.G. Callan and D.J. Gross. Phys. Rev. Lett. **22**, 156 (1969).

[4] V.N. Gribov and L.N. Lipatov, Sov. J. Nucl. Phys. 15 (1972) 438;
V.N. Gribov and L.N. Lipatov, Sov. J. Nucl. Phys. 15 (1972) 675;
L.N. Lipatov, Sov. J. Nucl. Phys. 20 (1975) 94;
Y.L. Dokshitzer, Sov. Phys. JETP 46 (1977) 641;
G. Altarelli and G. Parisi, Nucl. Phys. B 126 (1977) 298.

[5] F. Aaron *et al.* [H1 Collaboration] (2009), [arXiv:0904.0929].

[6] F. Aaron *et al.* [H1 Collaboration] (2009), [arXiv:0904.3513].

[7] C. Adloff *et al.* [H1 Collaboration], Eur. Phys. J. C **30**, 1 (2003).

[8] M. Botje, QCDNUM version 17β.

[9] R.S. Thorne and R.G. Roberts, Phys. Rev. **D57**, 6871 (1998).

[10] R.S. Thorne, Phys. Rev. **D73**, 054019 (2006).

[11] A. Glazov, AIP Conf. Proc. **792**, 237 (2005) [doi:10.1063/1.2122026].

[12] F.D. Aaron *et al.* [H1 and ZEUS Collaborations], Submitted to JHEP (2009), [arXiv:0911.0884].

[13] A. Benvenuti *et al.* [BCDMS Collaboration], Phys. Lett. **B223**, 485 (1989).

[14] M. Arneodo *et al.* [NMC Collaboration], Nucl. Phys. **B483**, 3 (1997).

[15] S. Chekanov *et al.* [ZEUS Collaboration], Phys. Lett. **B26255**, (2009).

[16] S. Chekanov *et al.* [ZEUS Collaboration], Eur. Phys. J. **C42**, 1 (2005).

[17] F. Aaron *et al.* [H1 Collaboration], Phys. Lett. B 665 (2008) 139.

[18] V. Chekelian [for the H1 Collaboration], Proc. of XVI Int. Workshop on Deep-Inelastic Scattering and Related Topics, London, England, April 2008 doi: 10.3360/dis.2008.39.

[19] S. Glazov [for the H1 Collaboration], Proc. of XVII Int. Workshop on Deep-Inelastic Scattering and Related Topics, Madrid, Spain, April 2009.

[20] S. Chekanov *et al.* [ZEUS Collaboration], EPJ **C62** 625 (2009).

[21] S. Chekanov *et al.* [ZEUS Collaboration], EPJ **C61** 223 (2009).

[22] F.D. Aaron *et al.* [H1 Collaboration], Submitted to EPJC, arxiv:0904.3870.

[23] F.D. Aaron *et al.* [H1 Collaboration]. Accepted by EPJC. arxiv:0907.2643.

[24] A. Airapetian *et al.* [HERMES Collaboration], Phys. Lett. **B666** 446 (2008).

Discussion

Benny Ward (Baylor University): What is the ultimate experimental precision on PDF's that you will achieve from all HERA data?
Answer: The expected precision is about 1%.